processes

MDPI

Article

Exploring Electrochemically Mediated ATRP of Styrene

Francesco De Bon [1,2], Gian Marco Carlan [1], Enrico Tognella [1] and Abdirisak Ahmed Isse [1,*]

[1] Department of Chemical Sciences, University of Padova, Via Marzolo 1, 35131 Padova, Italy; francesco.debon91@gmail.com (F.D.B.); gm.carlan@outlook.it (G.M.C.); enrico.tognella@studenti.unipd.it (E.T.)
[2] Centre for Mechanical Engineering Materials and Processes (CEMMPRE), Department of Chemical Engineering, University of Coimbra, Rua Sílvio Lima, Pólo II, 3030-790 Coimbra, Portugal
* Correspondence: abdirisak.ahmedisse@unipd.it

Abstract: Electrochemically mediated atom transfer radical polymerization (*e*ATRP) of styrene was studied in detail by using $CuBr_2$/TPMA (TPMA = tris(2-pyridylmethyl)amine) as a catalyst. Redox properties of various Cu(II) species were investigated in CH_3CN, dimethylformamide (DMF), and dimethyl sulfoxide (DMSO) both in the absence and presence of 50% (*v*/*v*) styrene. This investigation together with preliminary *e*ATRP experiments at 80 °C indicated DMF as the best solvent. The effects of catalyst, monomer, and initiator concentrations were also examined. The livingness of the polymerization was studied by chain extension and electrochemical temporal control of polymerization.

Keywords: styrene; *e*ATRP; temporal control; copper catalyst

Citation: De Bon, F.; Carlan, G.M.; Tognella, E.; Isse, A.A. Exploring Electrochemically Mediated ATRP of Styrene. *Processes* **2021**, *9*, 1327. https://doi.org/10.3390/pr9081327

Academic Editors: Carmen Boeriu, Francesca Lorandi and Sajjad Dadashi Silab

Received: 9 July 2021
Accepted: 28 July 2021
Published: 30 July 2021

1. Introduction

Atom transfer radical polymerization (ATRP) is one of the most preferred macromolecular engineering techniques owing to its facile setup, tolerance to a large extent of functional groups, often mild reaction conditions, and a vast number of applications [1,2]. Various ATRP techniques such as initiators for continuous activator regeneration (ICAR) ATRP [3,4], activators regenerated by electron transfer (ARGET) ATRP [5–8], supplemental activators and reducing agents (SARA) ATRP [9–12], photoATRP [13–15], photoinduced metal-free ATRP [16–18], electrochemically mediated ATRP (*e*ATRP) [19–24], and mechanoATRP [25–27] permitted facile and well-controlled polymerizations of a vast variety of monomers with low amounts of metal catalyst or with no metal catalyst at all.

A redox equilibrium involving a transition metal complex regulates the polymerization process, using various metals [28]. The most active and widely used catalysts are copper complexes with multidentate nitrogen-based ligands [29]. A general mechanism of copper-catalyzed ATRP with electrochemical regeneration of Cu^I activator complex is shown in Scheme 1. The process is initiated by an inner-sphere electron transfer involving the transfer of a halogen atom from an alkyl halide initiator, RX, or a halogen-capped dormant chain, P_n-X, to $[Cu^IL]^+$ (L = a nitrogen-based ligand), whereby the $[XCu^{II}L]^+$ deactivator and a carbon-centered radical are formed [30–32]. The latter propagates with a rate constant k_p by adding to a few monomer units before reacting with $[XCu^{II}L]^+$ to produce a dormant polymer chain and $[Cu^IL]^+$. Dormant polymers play a crucial role in controlled polymerizations [33]. A well-controlled polymerization requires the equilibrium to be strongly shifted to the left, with an equilibrium constant $K_{ATRP} = k_{act}/k_{deact} << 1$, to reduce the concentration of radicals and retain chain-end functionality. K_{ATRP} is generally very small in organic solvents but spans a wide range of values (10^{-4}–10^{-12}) because it is sensible to temperature, pressure, solvent, polymer chain-end structure, and type of catalyst [34–38]. Besides propagation with k_p and deactivation with k_{deact}, $P_n^\bullet$ can undergo termination reactions with a rate constant k_t. Although k_t is near the diffusion limit, the rate of termination reactions in ATRP is very low because of low $[P_n^\bullet]$ [1]. Nevertheless, continuous slow termination during

polymerization accumulates the catalyst in the deactivator form, i.e., $[XCu^{II}L]^+$, which must be reduced back to $[Cu^{I}L]^+$ to avoid reaction blockage. In electrochemically mediated ATRP, the activator form of the catalyst is regenerated by electrochemical reduction of $[XCu^{II}L]^+$ to $[Cu^{I}L]^+$ (Scheme 1).

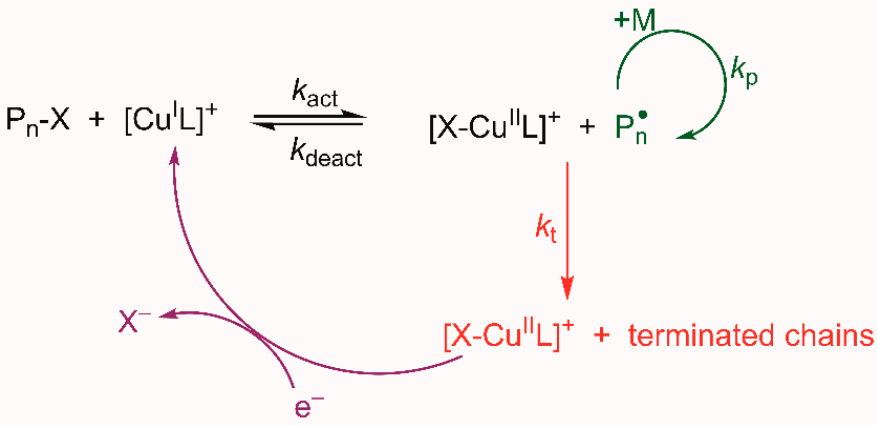

Scheme 1. Mechanism of ATRP with electrochemical regeneration of the activator complex (*e*ATRP).

Electrochemistry has demonstrated in the last years its extraordinary power in regenerating Cu^{I} species from Cu^{II} complexes, with the exclusive benefit of avoiding formation of by-products, as electrons are used *in lieu* of chemical reducing agents [23,24]. Furthermore, the ratio between Cu^{II} deactivator and Cu^{I} species is fixed by the applied potential, therefore it can be finely tuned by modulating the electrochemical stimulus. This technique, known as *e*ATRP was applied to several monomers in organic solvents, [39–46] water [47–54], miniemulsions [55–57], and ionic liquids [58,59].

Polystyrene (PS) is one of the most widely used plastics with a global production rate of several million tons per year. ATRP of styrene appeared for the first time in 1995 in the pioneering work of Matyjaszewski and Wang [60], and up to now it has been polymerized by almost all ATRP techniques, including conventional ATRP [60–62], ICAR ATRP [63–65], AGET and ARGET ATRP [8,66–70], SARA ATRP [71–74], and photo-induced ATRP [15,75–77]. Electrochemically mediated ATRP of styrene was instead not explored, apart from a preliminary study back in 2009 on Fe^{II}(Salen)-catalyzed polymerization, which appears to follow a reaction pathway involving an organometallic intermediate rather the typical ATRP mechanism [78]. It is known that styrene polymerization is hampered by its low propagation rate constant (k_p) [79] and usually high temperatures, typically above 100 °C, are used to polymerize it with a decent rate. This may appear to limit the possibility of *e*ATRP due to the harsh conditions to which the electrodes are exposed. Herein, we wish to show that *e*ATRP can be successfully applied to styrene. Our primary goal was to find an optimized set of conditions which provide polystyrene with a narrow molecular weight distribution and predefined molecular weight in a reasonably short time. The reaction was investigated in different solvents using $CuBr_2$/TPMA (TPMA = tris(2-pyridylmethyl)amine) as a catalyst and ethyl 2-bromoisobutyrrate (EBiB) as an initiator.

2. Materials and Methods

2.1. Materials

All solvents (DMF, CH_3CN, and DMSO, Sigma-Aldrich, Darmstadt, Germany) were of high purity and used without further purification. Copper(II) trifluoromethanesulfonate ($Cu(OTf)_2$, Sigma-Aldrich, Darmstadt, Germany, 98%), copper(II) bromide ($CuBr_2$, Sigma Aldrich, 99.999% trace metal basis), tris(2-pyridylmethyl)amine (TPMA, Sigma-Aldrich, Darmstadt, Germany, 98%), ethyl 2-bromoisobutyrrate (EBiB, Sigma Aldrich, Darmstadt, Germany, 98%), H_2SO_4 (Fluka, Buchs, Switzerland, 95%, TraceSELECT), tetrabutylammonium chloride (Bu_4NCl, Aldrich, Darmstadt, Germany, 98%), and tetrabutylammonium tetrafluoroborate (Bu_4NBF_4, Aldrich, Darmstadt, Germany, 98%) were used as received.

Styrene (Sigma-Aldrich, Darmstadt, Germany, >99%) was purified by passing through a column filled with active basic aluminum oxide (Al_2O_3, VWR chemicals, Milano, Italy) in the dark to remove polymerization inhibitors and stored at −20 °C in an amber bottle. Tetraethylammonium bromide (Et_4NBr, Sigma-Aldrich, Darmstadt, Germany, 99%) was recrystallized from acetone. Tetraethylammonium tetrafluoroborate (Et_4NBF_4, Alfa Aesar, Kandel, Germany, 99%) used as a supporting electrolyte was recrystallized twice from ethanol. After recrystallization, both salts were dried in a vacuum oven at 70 °C for 48 h.

2.2. Instrumentation

Electrochemical studies on the Cu catalyst were carried out in a 5-neck electrochemical cell, equipped with three electrodes, and connected to an Autolab PGSTAT 30 potentiostat/galvanostat (EcoChemie, Utrecht, The Netherlands) run by a PC with GPES software (EcoChemie). Electrosynthesis of polystyrene was carried out in a 5-neck electrochemical cell, equipped with three electrodes, connected to a PAR273A potentiostat/galvanostat (Princeton Applied Research, Oak Ridge, USA) run by a PC with Echem software. A glassy carbon (GC) disk, fabricated from a 3-mm diameter rod (Tokai GC-20, Tokyo, Japan), was used as a working electrode for cyclic voltammetry (CV). Before each experiment, the disk was cleaned by polishing with a 0.25-μm diamond paste, followed by ultrasonic rinsing in ethanol for 5 min. The working electrode employed for electrolysis was a Pt mesh (Alfa Aesar, Kandel, Germany, 99.9 % metals basis) with a geometric area of approximately 6 cm^2, which was electrochemically activated prior to each experiment by cycling the potential from −0.7 V to 1 V vs. $Hg\,|\,Hg_2SO_4$ at a scan rate of 0.2 V s^{-1} (60 cycles). The counter electrode was a Pt wire in CV, whereas a graphite rod was used for electrolysis. In the latter case, the electrode was separated from the working solution by a glass frit filled with the same electrolyte solution used in the working electrode compartment and a methylcellulose gel saturated with Et_4NBF_4. The reference electrode was $Ag\,|\,AgI\,|\,I^-$ 0.1 M *n*-Bu_4NI in DMF. Ferrocene (Fc) was added at the end of each experiment as an internal standard, so that all potentials are referred to the ferrocenium/ferrocene ($Fc^+\,|\,Fc$) redox couple. The cell was thermostated at 25 °C or 80 °C, and all experiments were performed under inert atmosphere (N_2 or Ar). The number average molecular weight (M_n) and dispersity ($Đ$) values were determined by gel permeation chromatography (GPC) with an Agilent 1260 Infinity GPC, equipped with a refractive index (RI) detector and two PLgel Mixed-D columns (300 mm, 5 μm) connected in series. The column compartment and RI detector were thermostated at 35 °C. The eluent was stabilized THF, at a flow rate of 1 mL/min. The column system was calibrated with 10 linear polystyrene (PS) standards (M_n = 162–371,100 Da). Monomer conversion was determined by ^{1}H-NMR spectroscopy with a 200 MHz Bruker Avance instrument, using $CDCl_3$ as a solvent.

2.3. Procedures

2.3.1. Typical Procedure for *e*ATRP of Styrene

The electrochemical cell was flushed with N_2 and loaded with 5 mL of DMF, 5 mL of styrene, 2.2 mg of $CuBr_2$, and 2.92 mg of TPMA under a flow of the inert gas. After heating the cell to 80 °C with a water bath, a CV of the catalyst was recorded to measure its standard reduction potential. Then 22 μL of EBiB was injected and a CV was recorded. Polymerization was started by applying the selected applied potential (E_{app}) and samples were withdrawn periodically to measure monomer conversion, and M_n and $Đ$ of the polymer.

2.3.2. Preparation of PS-Br Macroinitiator

A cell under N_2 flux was loaded with 2.5 mL of DMF, 2.2 mg of $CuBr_2$, 2.94 mg of TPMA, and 7.5 mL of styrene. After degassing the mixture with N_2 for at least 15 min, the cell was heated to 80 °C with a water bath and the CV was recorded. Then 22 μL of EBiB was injected and the CV was recorded. The polymerization was then started by applying $E_{app} = E_{1/2}$. The reaction was stopped after 2 h, and the polymer was precipitated into methanol and isolated by filtration. The polymer was washed twice with methanol

and dried under vacuum for several hours at 50 °C. The final weight PS-Br (M_n = 10,900, $Đ$ = 1.14), recovered as a white powder, was 1.0 g.

2.3.3. Procedure for Temporally Controlled *e*ATRP

The cell was prepared with all reagents as previously described for *e*ATRP of styrene. Polymerization was then started by applying $E_{app} = E_{1/2}$. After 1 h of reaction, the potential was set off and the cell remained disconnected from the electric circuit for 1 h after which $E_{app} = E_{1/2}$ was set again for 1 h, followed by another OFF period and a final 1 h of applied potential. Samples were withdrawn at the end of each step to measure monomer conversion, and molecular weight and $Đ$ of the polymer.

2.3.4. Chain Extension of PS-Br by *e*ATRP

The cell was prepared with all reagents as previously described for *e*ATRP of styrene except for using 0.2 g of PS-Br (M_n = 10,900, $Đ$ = 1.14) as a macroinitiator. Chain extension was performed by applying $E_{app} = E_{1/2}$ for 3 h. The final polymer had M_n = 24.9 kDa and $Đ$ = 1.17.

3. Results and Discussion

3.1. Voltammetric Behavior of the Catalyst

The copper catalyst is prepared in situ as $[BrCu^{II}TPMA]^+$ by mixing equimolar amounts of $CuBr_2$ and TPMA and the activator form, $[Cu^{I}TPMA]^+$, is electrogenerated during polymerization. To evaluate the redox properties of the catalyst and the relative stabilities of Cu^{II} and Cu^{I} complexes, both $[BrCu^{II}TPMA]^+$ and $[Cu^{II}TPMA]^{2+}$ were investigated by cyclic voltammetry (CV). The standard potentials of solvated copper ions were also estimated by cyclic voltammetry of $Cu(OTf)_2$ in the absence of added TPMA and Br^-. Typical CV responses of all investigated Cu^{II} species in DMF, DMSO, and CH_3CN as well as in 50% (*v*/*v*) solvent/styrene mixtures are reported in Figure 1. The observed peak couple stands for a one-electron transfer process involving the Cu^{II}/Cu^{I} redox couple. This allows easy determination of the standard potential as the half sum of the cathodic and anodic peak potentials, E_{pc} and E_{pa}, respectively: $E^\circ \approx E_{1/2} = (E_{pc} + E_{pa})/2$. The differences in current intensities are ascribed to changes of the diffusion coefficients of Cu^{II} species in different media.

The voltammetric pattern shown in Figure 1 did not change with the scan rate (v), except the current intensity which was proportional to $v^{1/2}$ and the separation between the cathodic and anodic peaks, which increased with increasing v. These findings clearly indicate that Cu^{II} undergoes a diffusion-controlled quasi-reversible electron transfer. Notably, although $\Delta E_p = E_{pc} - E_{pa}$ increased with increasing v, $E_{1/2}$ was independent of the scan rate. Therefore, E° was calculated for each redox couple as the average of the values measured at different scan rates in the range from 0.01 V/s to 1 V/s and the results are reported in Table 1. ΔE_p values measured at different scan rates were used to determine the standard rate constants of electron transfer (k°) for $[Cu^{II}TPMA]^{2+}$ and $[BrCu^{II}TPMA]^+$ according to the method of Nicholson [80]. k° values in the range 2.8×10^{-2}–1.0×10^{-1} cm/s were observed in pure solvents (Table 1). In general k° increased in the order DMSO < DMF < CH_3CN, roughly in agreement with the predicted dependence of k° on the longitudinal relaxation time of the solvent [81]. Addition of 50% styrene to the solvents decreased the standard rate constant of electron transfer.

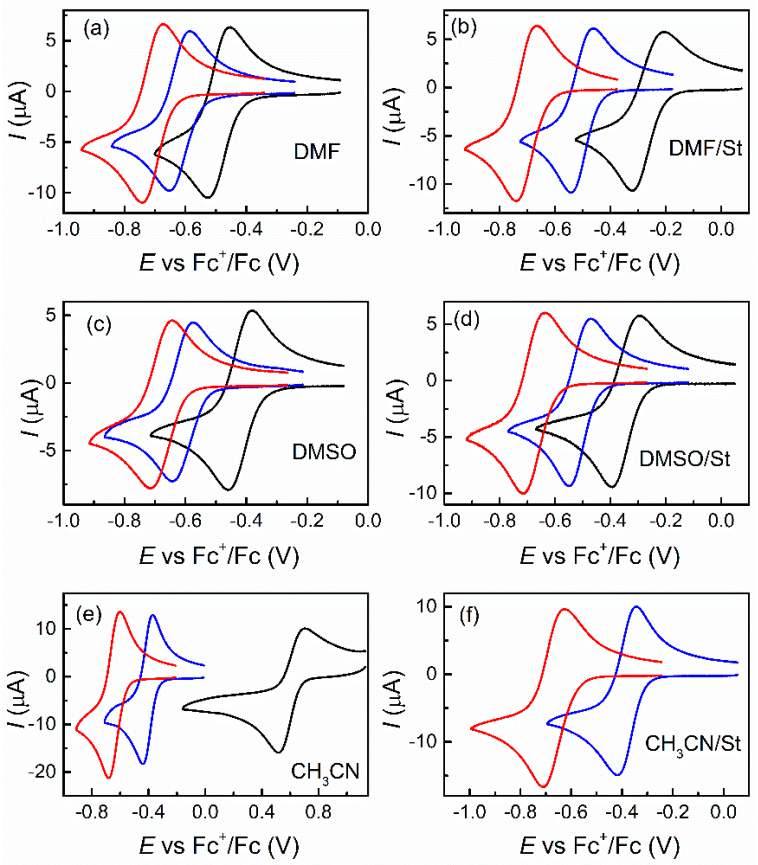

Figure 1. Cyclic voltammetry of 10^{-3} M $Cu^{II}(OTf)_2$ (—), $[Cu^{II}TPMA]^{2+}$ (—) and $[BrCu^{II}TPMA]^+$ (—) in pure solvents (**a**,**c**,**e**) and 50% (*v*/*v*) solvent/styrene mixtures (**b**,**d**,**f**)) containing 0.1 M Et_4NBF_4 as a supporting electrolyte, recorded on a GC electrode at 0.1 V/s and T = 25 °C.

Table 1. Redox properties of copper complexes and their relative stabilities in different media at 25 °C.

Solvent [1]	Cu(II)	E° [2] (V)	$10^2 \times k^\circ$ (cm s^{-1})	β^{II}/β^{I}	$K_{Br}{}^{II}/K_{Br}{}^{I}$
DMF	$Cu(OTf)_2$	−0.486			
DMF	$[CuTPMA]^{2+}$	−0.621	2.8	1.89×10^2	
DMF	$[BrCuTPMA]^+$	−0.708	4.4		29.9
DMSO	$Cu(OTf)_2$	−0.418			
DMSO	$[CuTPMA]^{2+}$	−0.615	1.6	2.14×10^3	
DMSO	$[BrCuTPMA]^+$	−0.687	2.3		16.5
CH_3CN	$Cu(OTf)_2$	0.611			
CH_3CN	$[CuTPMA]^{2+}$	−0.408	7.5	1.67×10^{17}	
CH_3CN	$[BrCuTPMA]^+$	−0.658	10		1.69×10^4
DMF/St	$Cu(OTf)_2$	−0.266			
DMF/St	$[CuTPMA]^{2+}$	−0.505	0.8	1.10×10^4	
DMF/St	$[BrCuTPMA]^+$	−0.710	3.0		2.92×10^3
DMSO/St	$Cu(OTf)_2$	−0.346			
DMSO/St	$[CuTPMA]^{2+}$	−0.514	0.7	6.92×10^2	
DMSO/St	$[BrCuTPMA]^+$	−0.693	2.4		1.05×10^3
CH_3CN/St	$Cu(OTf)_2$	-		-	
CH_3CN/St	$[CuTPMA]^{2+}$	−0.384	1.6		
CH_3CN/St	$[BrCuTPMA]^+$	−0.683	7.4		1.13×10^5

[1] St = styrene; solvent/monomer mixtures were 50/50 (*v*/*v*). [2] vs Fc^+/Fc couple.

The standard reduction potentials of Cu^{2+}, $[Cu^{II}TPMA]^{2+}$, and $[BrCu^{II}TPMA]^{+}$ can be used to evaluate the relative stabilities of Cu^{I} and Cu^{II} complexes with TPMA and their relative affinities for Br^{-}, according to Equations (1) and (2):

$$E^{o}_{[Cu^{II}L]^{2+}/[Cu^{I}L]^{+}} = E^{o}_{Cu^{2+}/Cu^{+}} - \frac{RT}{F}\ln\frac{\beta^{II}}{\beta^{I}} \quad (1)$$

$$E^{o}_{[BrCu^{II}L]^{+}/[BrCu^{I}L]} = E^{o}_{[Cu^{II}L]^{2+}/[Cu^{I}L]^{+}} - \frac{RT}{F}\ln\frac{K^{II}_{Br}}{K^{I}_{Br}} \quad (2)$$

where β^{I} and β^{II} are the stability constants of $[Cu^{I}TPMA]^{+}$ and $[Cu^{II}TPMA]^{2+}$, respectively, defined as the formation equilibrium constants of the complexes from the solvated copper ions and the ligand. ${K_{Br}}^{II}$ and ${K_{Br}}^{I}$ are the binding constants of Br^{-} to $[Cu^{II}TPMA]^{2+}$ and $[Cu^{I}TPMA]^{+}$, respectively; they express the halidophilicities of the $Cu^{II/I}$/TPMA complexes. This type of analysis was previously applied to $Cu^{II/I}$/TPMA complexes but was limited to the determination of ${K_{Br}}^{II}/{K_{Br}}^{I}$ in pure solvents [82]. Here, we consider both pure solvents and solvent/styrene mixtures and extend the analysis to the calculation of β^{II}/β^{I}. Calculated values of β^{II}/β^{I} and ${K_{Br}}^{II}/{K_{Br}}^{I}$ are listed in Table 1. In all reaction media, $\beta^{II} >> \beta^{I}$ but neither the effect of solvent type nor that of 50 vol% of styrene can be easily rationalized. Moreover, ${K_{Br}}^{II}$ is always greater than ${K_{Br}}^{I}$ and the higher affinity of Br^{-} for $[Cu^{II}TPMA]^{2+}$ than $[Cu^{I}TPMA]^{+}$ further increases in the presence of styrene. This is particularly important because it is desirable to have a deactivator complex ($[XCu^{II}L]^{+}$) with good stability while the activator complex should not have high affinity for halide ions to avoid speciation of Cu^{I} to produce inactive species [30,83].

The β^{II}/β^{I} and ${K_{Br}}^{II}/{K_{Br}}^{I}$ values of Table 1 can be used to calculate the values of β^{II}, β^{I} ${K_{Br}}^{II}$, and ${K_{Br}}^{I}$ provided that one of the values in each ratio is known. Unfortunately, there are no data on the stability constants, whereas some values of ${K_{Br}}^{II}$ in pure solvents are available in the literature. Zerk and Bernhardt [84] reported ${K_{Br}}^{II}$ values of 3.47×10^{7} M^{-1} and 1.1×10^{5} M^{-1} in CH_3CN and DMSO, respectively, whereas Fantin et al. [85] reported ${K_{Br}}^{II} = 4.2 \times 10^{5}$ M^{-1} in DMF. These values give ${K_{Br}}^{I} = 1.4 \times 10^{4}$ M^{-1}, 6.7×10^{2} M^{-1} and 2.0×10^{3} M^{-1} in DMF, DMSO, and CH_3CN, respectively.

3.2. Electrochemically Mediated ATRP of Styrene

All polymerizations were carried out at $T = 80$ °C to guarantee a decent polymerization rate. The catalyst was $[BrCu^{II}TPMA]^{+}$, prepared in situ by mixing equimolar amounts of $CuBr_2$ and TPMA in the chosen solvent/styrene mixture. Ethyl α-bromoisobutyrate (EBiB) was used as an initiator. Before starting the polymerization, cyclic voltammetry of the system was always performed on a glassy carbon electrode to measure the formal reduction potential of the catalyst and evaluate the effect of the initiator. Figure 2 shows an example of the voltammetric behavior of $[BrCu^{II}TPMA]^{+}$ in the presence of excess initiator. Addition of EBiB in a 15-fold excess with respect to the catalyst considerably changed the voltammetric response: the cathodic peak increased, while the anodic one almost disappeared. These changes are consistent with the catalytic activation of the initiator by electrogenerated Cu^{I}. Reduction of $[BrCu^{II}TPMA]^{+}$ at the electrode produces $[BrCu^{I}TPMA]$ (Equation (3)), which partially dissociates to give the activator form of the catalyst, $[Cu^{I}TPMA]^{+}$ (Equation (4)). Reaction of the latter with the initiator EBiB regenerates the starting Cu^{II} species together with a radical (Equation (5)), which either terminates by radical-radical coupling and disproportionation or is deactivated after a short period of propagation. During a cyclic voltammetry experiment, these reactions occur in a thin reaction layer adjacent to the electrode. Therefore, the Cu^{II} species generated by reaction 5, easily reaches the electrode where it is reduced again to Cu^{I} (Equation (3)). Depending on the kinetics of the activation reaction, this sequence may be repeated several times, leading to an increase of the cathodic peak current and a decrease or disappearance of the anodic one.

$$\left[\mathrm{BrCu^{II}TPMA}\right]^{+} + \mathrm{e}^{-} \rightleftarrows \left[\mathrm{BrCu^{I}TPMA}\right] \quad (3)$$

$$\left[\mathrm{BrCu^{I}TPMA}\right] \rightleftarrows \left[\mathrm{Cu^{I}TPMA}\right]^{+} + \mathrm{Br}^{-} \quad (4)$$

$$\left[\mathrm{Cu^{I}TPMA}\right]^{+} + \mathrm{RBr} \rightleftarrows \left[\mathrm{BrCu^{II}TPMA}\right]^{+} + \mathrm{R}^{\bullet} \quad (5)$$

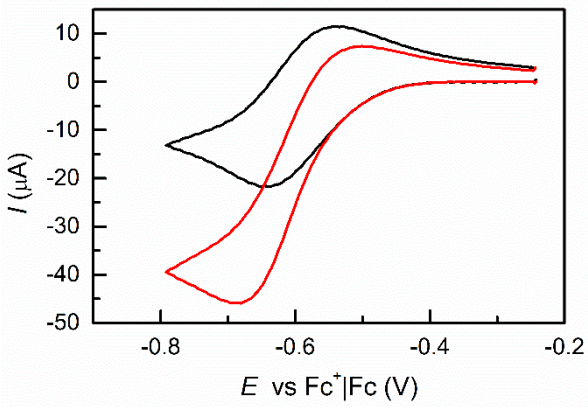

Figure 2. Cyclic voltammetry of 10^{-3} M $[BrCu^{II}TPMA]^{+}$ in DMF/styrene (50:50, *v*/*v*) + 0.1 M Et_4NBF_4 in the absence (—) and presence of 1.5×10^{-2} M EBiB (—), recorded on a GC disk electrode at 0.2 V/s and T = 80 °C.

3.2.1. Effect of the Solvent

Since *e*ATRP of styrene has never been investigated, the effect of the solvent was first evaluated. The results of a first set of *e*ATRP experiments are summarized in Table 2. All experiments were performed under potentiostatic control with an applied potential $E_{app} = E_{1/2} \approx E^{\circ}$ of the $[BrCu^{II}TPMA]^{+}/[BrCu^{I}TPMA]$ couple. First-order kinetic plots and evolution of molecular weight and dispersity in CH_3CN and DMF are shown in Figure 3, together with an example of typical molecular weight distributions of the obtained PS-Br polymer.

Table 2. Potentiostatic *e*ATRP of 50% (*v*/*v*) styrene in different solvents at T = 80 °C [1].

Entry	Solvent	t (h)	Q (C)	Conversion (%)	$10^2 \times k_p^{app}$ [2] (h^{-1})	$M_{n,th}$ [3] (kDa)	M_n [4] (kDa)	$Đ$
1	DMF	5	5.82	34	8.7	10.5	10.6	1.26
2	DMSO	2	0.99	15	- [5]	4.7	4.8	1.22
3	CH_3CN	4	3.39	47	17.1	14.4	17.2	1.37

[1] Other conditions: [St]:[EBiB]:[Catalyst] = 435:1.5:0.1; DP = 291; $[Cu^{II}]$ = 1 mM; $E_{app} = E_{1/2}$; V_{tot} = 10 mL; 0.1 M Et_4NBF_4 supporting electrolyte. [2] Apparent rate constant of polymerization, determined as the slope of $\ln([St]_0/[St])$ vs t. [3] Theoretical molecular weight, calculated as $M_{n,th} = M_{EBiB}$ + conversion × DP × M_{St}. [4] Determined by GPC. [5] Not determined because of polymer precipitation.

Although the reaction was well-controlled in all three solvents, significant differences were observed in the overall performance of the process. The polymerization was fastest in CH_3CN, reaching 47% conversion in 4 h, but the polymer started precipitating at this stage and therefore the reaction had to be stopped. Additionally, dispersity slightly increased with conversion, passing from 1.17 to 1.37 as the conversion increased from 22% to 47%. Another disadvantage of CH_3CN is its relatively low boiling point (82 °C), causing some technical issues related to solvent evaporation at the chosen polymerization temperature of 80 °C. The reaction was also fast in DMSO, but even low molecular weight polystyrene is insoluble in this solvent and the process had to be stopped after only 1 h of polymerization with 15% conversion when solid PS separated from the reaction mixture. Polymerization

was slowest in DMF, but the reaction proceeded with good control and did not present solubility issues. GPC traces taken during *e*ATRP in DMF were symmetrical without tailing and continuously shifted to higher molecular weights with increasing conversion (Figure 3c). Therefore, this solvent was chosen for further investigations on *e*ATRP of styrene. The effects of monomer concentration, catalyst loading, and targeted degree of polymerization were examined.

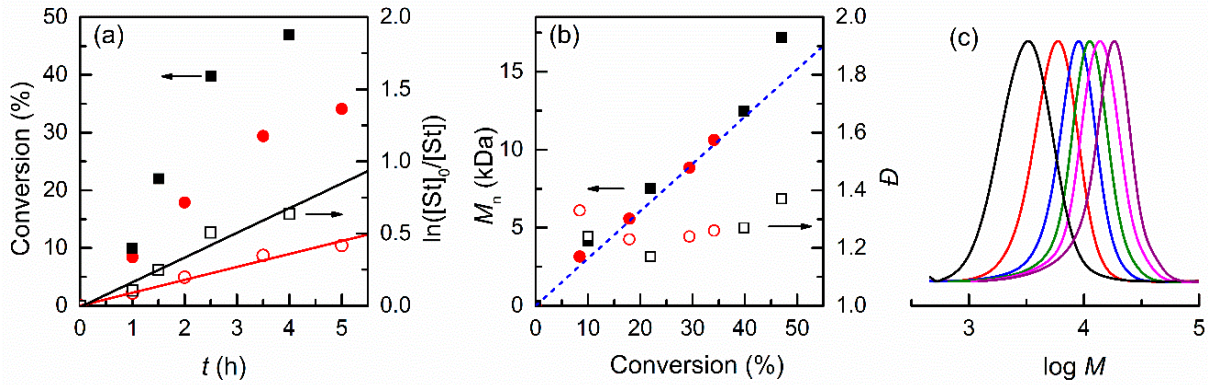

Figure 3. (**a**) First-order kinetic plots and (**b**) evolution of M_n and $Đ$ with conversion for potentiostatic *e*ATRP of styrene in DMF (circles) or CH_3CN (squares), performed at 80 °C at $E_{app} = E_{1/2}$ with [St]:[EBiB]:[Catalyst] = 435:1.5:0.1; DP = 291; $[Cu^{II}]$ = 1 mM. The dashed line in (**b**) represents theoretical molecular weights. (**c**) Molecular weight distributions of PS-Br produced by *e*ATRP of 50% (*v*/*v*) styrene in DMF.

3.2.2. Effect of Initiator and Concentrations of Catalyst and Monomer in DMF

Table 3 shows the results of *e*ATRP of styrene carried out in DMF at different conditions. The effect of the initiator concentration was first investigated. Keeping constant both monomer and catalyst concentrations, the quantity of EBiB was lowered from 15 mM down to 2 mM, which corresponds to an increase of target degree of polymerization (DP) from 290 to 2175 (Table 3, entries 1–3). In this set of polymerizations, the reaction was stopped when $Đ$ became higher than 1.3. Polymerizations were well-controlled as evidenced by the trends shown in Figure 4, but the overall rate of the reaction decreased as the concentration of the initiator was lowered. This led to a decrease of monomer conversion from 34% to 6.3%. However, high molecular weight PS could be prepared when high DP was targeted.

Next, the concentration of the catalyst was lowered from 1 mM to 0.2 mM (Table 3, entries 3–7), keeping the initiator concentration at 2 mM to prepare high molecular weight PS. Lowering the catalyst load is important to improve the cleanness of the system and a slight improvement of process performance was observed. Compared to *e*ATRP with 1 mM copper (Table 3, entry 3), monomer conversion after 2 h increased to 7.7% and 8.8% when the catalyst concentration was lowered to 0.5 mM and 0.2 mM, respectively. In all cases the dispersity of the obtained polymer was ~1.3. When the reactions with 0.5 mM and 0.2 mM catalyst were protracted up to 4 h, conversions further increased to 11.4% and 12.5% yielding PS with M_n = 26.6 kDa and 31.9, respectively. However, in both cases the dispersity worsened reaching 1.46 and 1.52 at $[Cu^{II}]$ = 0.5 mM and 0.2 mM, respectively.

Last, a series of *e*ATRPs with different amounts of monomer (25%, 50%, and 75% (*v*/*v*)) was carried out under otherwise identical conditions, i.e., $[Cu^{II}]$ = 1 mM, [EBiB] = 15 mM, T = 80 °C (Table 3, entries 1, 8, and 9). In all monomer/solvent ratios (1:3–3:1, *v*/*v*) polymerization proceeded in a well-controlled manner as attested by the low values of dispersity and the excellent match between experimental molecular weights and theoretical values (Figure 5). Interestingly, the monomer concentration had a noticeable effect on the polymerization rate. The apparent propagation rate constant, k_p^{app}, increased from 2.4×10^{-2} h^{-1} to 0.10 h^{-1} when the initial styrene concentration was changed from 25% to 75% (*v*/*v*). This suggests that increasing the amount of styrene in the reaction mixture could be an efficient strategy to address the slow polymerization kinetics of the monomer.

Table 3. Potentiostatic *e*ATRP of styrene in DMF initiated by EBiB at 80 °C [1].

Entry	St (vol%)	[Cu^{II}] (mM)	[EBiB] (mM)	DP	*t* (h)	*Q* (C)	Conversion (%)	$10^2 \times k_p^{app}$ [2] (h^{-1})	$M_{n,th}$ [3] (kDa)	M_n [4] (kDa)	*Đ*
1	50	1.0	15	290	5	5.8	34	8.7	10.5	10.7	1.26
2	50	1.0	7.5	580	4	7.7	11	2.9	6.7	5.6	1.33
3	50	1.0	2	2175	2	2.5	6.3	3.1	14.5	14.1	1.33
4	50	0.5	2	2175	2	2.6	7.7	3.0	17.6	19.1	1.32
5	50	0.5	2	2175	4	3.5	11.4	3.0	26.0	26.6	1.46
6	50	0.2	2	2175	2	1.4	8.8	3.4	20.2	24.3	1.32
7	50	0.2	2	2175	4	1.9	12.5	3.4	28.5	31.9	1.52
8	25	1.0	15	145	5	3.1	13	2.4	2.1	2.3	1.35
9	75	1.0	15	435	5	10.1	40	10.0	18.3	19.4	1.29

[1] Other conditions: $E_{app} = E_{1/2}$; V_{tot} = 10 mL; supporting electrolyte (Et_4NBF_4): 0.1 M (entries 1 and 2) or 0.2 M (entry 3). [2] Apparent rate constant of polymerization, determined as the slope of $\ln([St]_0/[St])$ vs *t*. [3] Theoretical molecular weight, calculated as $M_{n,th} = M_{EBiB}$ + conversion × DP × M_{St}. [4] Determined by GPC.

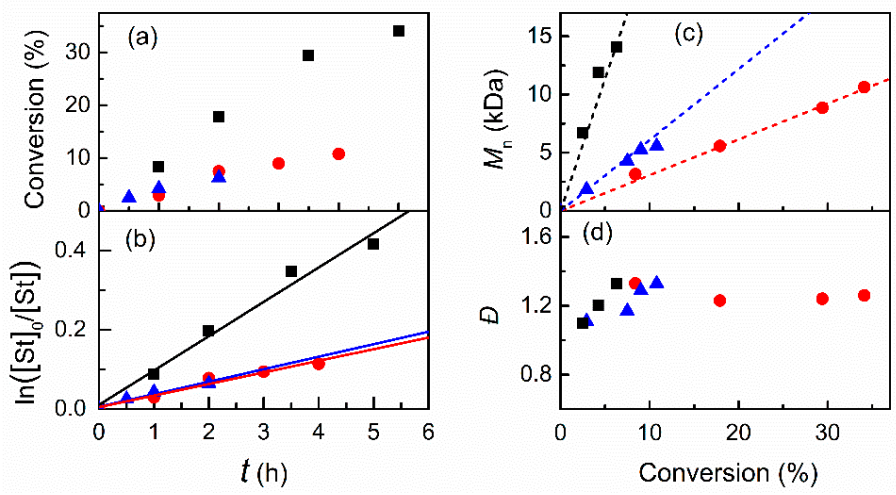

Figure 4. (**a**) Conversion, (**b**) kinetic plots and evolution of (**c**) M_n and (**d**) *Đ* with conversion for potentiostatic *e*ATRP of 50% (*v*/*v*) styrene in DMF at $E_{app} = E_{1/2}$. For reaction conditions refer to Table 3, entry: 1 (■), 2 (●) and 3 (▲) and. The dashed lines in (**c**) represent the theoretical molecular weight.

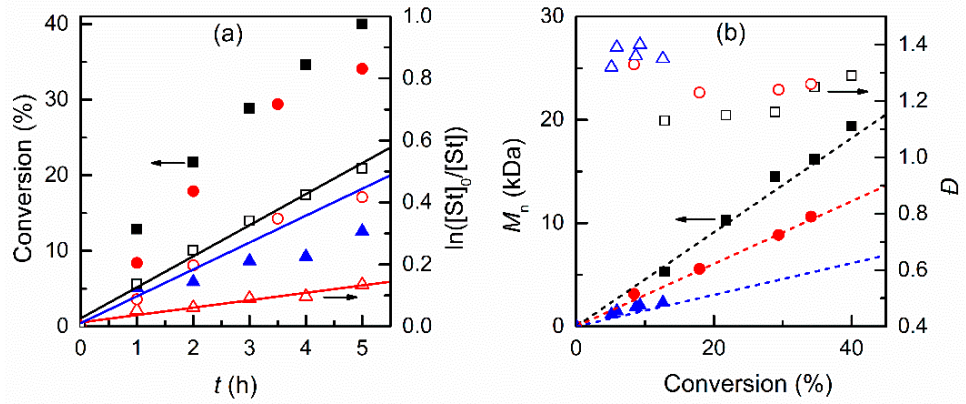

Figure 5. (**a**) Kinetic plots and (**b**) evolution of M_n and *Đ* with conversion for potentiostatic *e*ATRP of styrene in DMF at St/DMF (*v*/*v*) = 75/25 (squares), 50/50 (circles) and 25/75 (triangles); other conditions: [St]:[EBiB]:[Catalyst] = *x*:1.5:0.1, where *x* = 654, 435, and 218; [Cu^{II}] = 10^{-3} M; $E_{app} = E_{1/2}$; *T* = 80 °C. The dashed lines in (**b**) represent the theoretical molecular weights.

The effect of monomer concentration on the polymerization rate is more marked by passing from 25 to 50% than from 50 to 75% (*v*/*v*). First-order kinetics and linear evolution of M_n with conversion were observed in all cases. Dispersity, however, was slightly better when polymerization was carried out above 25% (*v*/*v*) styrene. In terms of polymer molecular weight, the best results were obtained when styrene was polymerized at 75% (*v*/*v*) monomer, albeit the use of excess supporting electrolyte to improve the conductivity of the mixture. Therefore, polymerizing at 75% (*v*/*v*) styrene produces more polymer per batch, amortizing the cost of the expensive electrolyte.

3.3. Temporal Control of Polymerization

Temporal control in *e*ATRP can be easily achieved by appropriately adjusting the applied potential, E_{app}, so that polymerization can be triggered, stopped, and then restarted when desired [19,58]. The electrochemical switch can be designed in two different ways: (i) intermittent switching between two E_{app} values, one for electrochemical (re)generation of the activator and the other for its rapid oxidation, and (ii) a fixed E_{app} value appropriate for activator (re)generation with toggling of the electrochemical cell between ON and OFF positions. The first approach has been widely tested showing that virtually no polymerization occurs during the OFF period because all Cu^I species in the solution are rapidly oxidized to Cu^{II}. We focused on the second approach, which has never been tested although it is conceptually simpler than the first. *e*ATRP of 75% (*v*/*v*) styrene in DMF (Table 3, entry 9) was repeated by applying $E_{app} = E_{1/2}$ for three 1-h steps interposed by two 1-h steps in which the cell was switched off. As shown in Figure 6a, during the periods of catalyst activation by electroreduction, 7–11% monomer conversion could be achieved, whereas further increase of conversion was <1% during 1 h when the cell was switched off. Polymerization was always well-controlled producing a polymer with very narrow molecular weight distribution (Figure 6b). Additionally, M_n increased linearly with conversion, closely matching the theoretical values, each time the polymerization was triggered after a period of almost inactivity in which there was no applied potential, clearly indicating a good chain-end fidelity. Interestingly, temporal control in *e*ATRP works very well without toggling between two values of E_{app} as is usually done. When the cell was switched off, the reaction continued at a very reduced rate with <1% monomer conversion in 1 h as compared to 7–11% obtained when current was circulated in the cell. This points out that the effective concentration of Cu^I in solution during *e*ATRP is quite low and when the continuous regeneration is stopped, the polymerization rate drops rapidly and eventually the reaction stops.

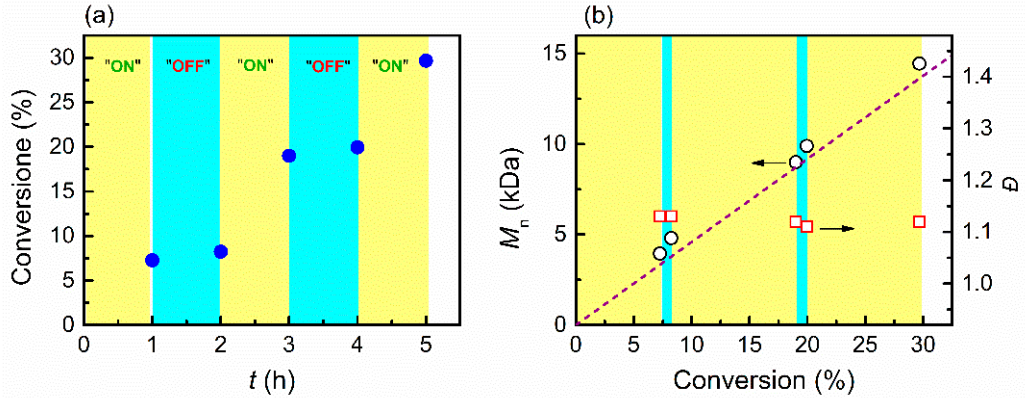

Figure 6. (**a**) Kinetic plots and (**b**) evolution of M_n and $Đ$ with conversion for potentiostatic *e*ATRP of 75% (*v*/*v*) styrene in DMF at $E_{app} = E_{1/2}$. Conditions: [St]:[EBiB]:[Catalyst] = 654:1.5:0.1; $[Cu^{II}] = 10^{-3}$ M. The dashed line represents the theoretical molecular weight.

3.4. Electrochemical Chain Extension

The livingness of the polymerization was demonstrated also by chain extension from a PS-Br macroinitiator. To this end, *e*ATRP of 75% (v/v) styrene in DMF was carried at $E_{app} = E_{1/2}$ for 2 h to prepare a PS-Br macroinitiator with M_n = 10.9 kDa and $Đ$ = 1.14 (see materials and methods). After isolation and purification, the polymer was used as a macroinitiator in a second *e*ATRP experiment conducted in 75% (v/v) styrene in DMF at $E_{app} = E_{1/2}$. A clear shift of the molecular weight distribution was observed after the extension experiment (Figure 7). The GPC trace remained monomodal showing no dead chains in the macroinitiator or during the chain extension.

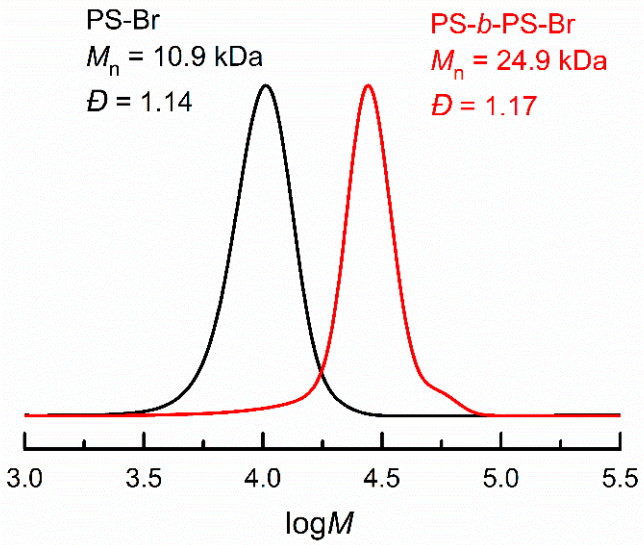

Figure 7. Molecular weight distributions of PS-Br macroinitiator (▬) and PS-*b*-PS-Br homopolymer (▬) after chain extension by *e*ATRP of 75% (v/v) styrene in DMF at T = 80 °C and $E_{app} = E_{1/2}$.

4. Conclusions

Electrochemically mediated ATRP of styrene was studied in detail by varying a series of parameters such as monomer amount, solvent, degree of polymerization, and catalyst concentration. DMF was the best solvent among the three polar solvents chosen for this study, namely DMF, DMSO, and CH_3CN. We determined that best polymerizations take place when the monomer amount is beyond 50% (v/v) at T = 80 °C in DMF. The livingness of the polymerization was verified via chain extension from PS-Br macroinitiator, with styrene, affording a controlled PS-*b*-PS-Br linear homopolymer. Livingness was also confirmed by excellent temporal control of polymerization, achieved by toggling between active *e*ATRP via $E_{app} = E_{1/2}$ and interruption of current passage to stop the reaction. This study shows that *e*ATRP of styrene at 80 °C is a well-controlled process, but monomer conversion is limited because of the slow propagation rate of styrene. The electrochemical method is, however, appropriate for the preparation of medium molecular weight polymers in few hours at a moderate temperature.

Author Contributions: Conceptualization, A.A.I. and F.D.B.; methodology, A.A.I. and F.D.B.; investigation, G.M.C., E.T., and F.D.B.; supervision: A.A.I. and F.D.B.; data curation: all authors; writing—original draft preparation, A.A.I. and F.D.B.; writing—review and editing, A.A.I. and F.D.B. All authors have read and agreed to the published version of the manuscript.

Funding: This research received no external funding.

Institutional Review Board Statement: Not applicable.

Informed Consent Statement: Not applicable.

Data Availability Statement: All data collected in this study are contained within the article.

Acknowledgments: F.D.B acknowledges sponsoring by national funds through FCT—Fundação para Ciência e Tecnologia—under the project UIDB/00285/2020.

Conflicts of Interest: The authors declare no conflict of interest.

References

1. Matyjaszewski, K. Atom Transfer Radical Polymerization (ATRP): Current Status and Future Perspectives. *Macromolecules* **2012**, *45*, 4015–4039. [CrossRef]
2. Matyjaszewski, K.; Gao, H.; Sumerlin, B.S.; Tsarevsky, N.V. (Eds.) *Reversible Deactivation Radical Polymerization: Materials and Applications*; ACS Symposium Series; American Chemical Society: Washington, DC, USA, 2018; Volume 1285, ISBN 9780841233232.
3. Matyjaszewski, K.; Jakubowski, W.; Min, K.; Tang, W.; Huang, J.; Braunecker, W.A.; Tsarevsky, N.V. Diminishing Catalyst Concentration in Atom Transfer Radical Polymerization with Reducing Agents. *Proc. Natl. Acad. Sci. USA* **2006**, *103*, 15309–15314. [CrossRef] [PubMed]
4. Konkolewicz, D.; Magenau, A.J.D.; Averick, S.E.; Simakova, A.; He, H.; Matyjaszewski, K. ICAR ATRP with Ppm Cu Catalyst in Water. *Macromolecules* **2012**, *45*, 4461–4468. [CrossRef]
5. Min, K.; Gao, H.; Matyjaszewski, K. Use of Ascorbic Acid as Reducing Agent for Synthesis of Well-Defined Polymers by ARGET ATRP. *Macromolecules* **2007**, *40*, 1789–1791. [CrossRef]
6. Chan, N.; Cunningham, M.F.; Hutchinson, R.A. ARGET ATRP of Methacrylates and Acrylates with Stoichiometric Ratios of Ligand to Copper. *Macromol. Chem. Phys.* **2008**, *209*, 1797–1805. [CrossRef]
7. Simakova, A.; Averick, S.E.; Konkolewicz, D.; Matyjaszewski, K. Aqueous ARGET ATRP. *Macromolecules* **2012**, *45*, 6371–6379. [CrossRef]
8. Mendonça, P.V.; Ribeiro, J.P.M.; Abreu, C.M.R.; Guliashvili, T.; Serra, A.C.; Coelho, J.F.J. Thiourea Dioxide As a Green and Affordable Reducing Agent for the ARGET ATRP of Acrylates, Methacrylates, Styrene, Acrylonitrile, and Vinyl Chloride. *ACS Macro Lett.* **2019**, *8*, 315–319. [CrossRef]
9. Abreu, C.M.R.; Serra, A.C.; Popov, A.V.; Matyjaszewski, K.; Guliashvili, T.; Coelho, J.F.J. Ambient Temperature Rapid SARA ATRP of Acrylates and Methacrylates in Alcohol–Water Solutions Mediated by a Mixed Sulfite/Cu(II)Br_2 Catalytic System. *Polym. Chem.* **2013**, *4*, 5629. [CrossRef]
10. Mendes, J.P.; Branco, F.; Abreu, C.M.R.; Mendonça, P.V.; Serra, A.C.; Popov, A.V.; Guliashvili, T.; Coelho, J.F.J. Sulfolane: An Efficient and Universal Solvent for Copper-Mediated Atom Transfer Radical (Co)Polymerization of Acrylates, Methacrylates, Styrene, and Vinyl Chloride. *ACS Macro Lett.* **2014**, *3*, 858–861. [CrossRef]
11. Lorandi, F.; Fantin, M.; Isse, A.A.; Gennaro, A. RDRP in the Presence of Cu^0: The Fate of Cu(I) Proves the Inconsistency of SET-LRP Mechanism. *Polymer* **2015**, *72*, 238–245. [CrossRef]
12. Kopeć, M.; Yuan, R.; Gottlieb, E.; Abreu, C.M.R.; Song, Y.; Wang, Z.; Coelho, J.F.J.; Matyjaszewski, K.; Kowalewski, T. Polyacrylonitrile- b -Poly(Butyl Acrylate) Block Copolymers as Precursors to Mesoporous Nitrogen-Doped Carbons: Synthesis and Nanostructure. *Macromolecules* **2017**, *50*, 2759–2767. [CrossRef]
13. Tasdelen, M.A.; Uygun, M.; Yagci, Y. Photoinduced Controlled Radical Polymerization. *Macromol. Rapid Commun.* **2011**, *32*, 58–62. [CrossRef] [PubMed]
14. Konkolewicz, D.; Schröder, K.; Buback, J.; Bernhard, S.; Matyjaszewski, K. Visible Light and Sunlight Photoinduced ATRP with Ppm of Cu Catalyst. *ACS Macro Lett.* **2012**, *1*, 1219–1223. [CrossRef]
15. Anastasaki, A.; Nikolaou, V.; Zhang, Q.; Burns, J.; Samanta, S.R.; Waldron, C.; Haddleton, A.J.; McHale, R.; Fox, D.; Percec, V.; et al. Copper(II)/Tertiary Amine Synergy in Photoinduced Living Radical Polymerization: Accelerated Synthesis of ω-Functional and α,ω-Heterofunctional Poly(Acrylates). *J. Am. Chem. Soc.* **2014**, *136*, 1141–1149. [CrossRef]
16. Treat, N.J.; Sprafke, H.; Kramer, J.W.; Clark, P.G.; Barton, B.E.; Read de Alaniz, J.; Fors, B.P.; Hawker, C.J. Metal-Free Atom Transfer Radical Polymerization. *J. Am. Chem. Soc.* **2014**, *136*, 16096–16101. [CrossRef]
17. Yilmaz, G.; Yagci, Y. Photoinduced Metal-Free Atom Transfer Radical Polymerizations: State-of-the-Art, Mechanistic Aspects and Applications. *Polym. Chem.* **2018**, *9*, 1757–1762. [CrossRef]
18. Pan, X.; Fang, C.; Fantin, M.; Malhotra, N.; So, W.Y.; Peteanu, L.A.; Isse, A.A.; Gennaro, A.; Liu, P.; Matyjaszewski, K. Mechanism of Photoinduced Metal-Free Atom Transfer Radical Polymerization: Experimental and Computational Studies. *J. Am. Chem. Soc.* **2016**, *138*, 2411–2425. [CrossRef] [PubMed]
19. Magenau, A.J.D.; Strandwitz, N.C.; Gennaro, A.; Matyjaszewski, K. Electrochemically Mediated Atom Transfer Radical Polymerization. *Science* **2011**, *332*, 81–84. [CrossRef]
20. Magenau, A.J.D.; Bortolamei, N.; Frick, E.; Park, S.; Gennaro, A.; Matyjaszewski, K. Investigation of Electrochemically Mediated Atom Transfer Radical Polymerization. *Macromolecules* **2013**, *46*, 4346–4353. [CrossRef]
21. Lorandi, F.; Fantin, M.; Isse, A.A.; Gennaro, A. Electrochemically Mediated Atom Transfer Radical Polymerization of N-Butyl Acrylate on Non-Platinum Cathodes. *Polym. Chem.* **2016**, *7*, 5357–5365. [CrossRef]
22. Fantin, M.; Lorandi, F.; Isse, A.A.; Gennaro, A. Sustainable Electrochemically-Mediated Atom Transfer Radical Polymerization with Inexpensive Non-Platinum Electrodes. *Macromol. Rapid Commun.* **2016**, *37*, 1318–1322. [CrossRef] [PubMed]
23. Chmielarz, P.; Fantin, M.; Park, S.; Isse, A.A.; Gennaro, A.; Magenau, A.J.D.; Sobkowiak, A.; Matyjaszewski, K. Electrochemically Mediated Atom Transfer Radical Polymerization (*e*ATRP). *Prog. Polym. Sci.* **2017**, *69*, 47–78. [CrossRef]

24. Lorandi, F.; Fantin, M.; Isse, A.A.; Gennaro, A. Electrochemical Triggering and Control of Atom Transfer Radical Polymerization. *Curr. Opin. Electrochem.* **2018**, *8*, 1–7. [CrossRef]
25. Mohapatra, H.; Kleiman, M.; Esser-Kahn, A.P. Mechanically Controlled Radical Polymerization Initiated by Ultrasound. *Nat. Chem.* **2017**, *9*, 135–139. [CrossRef]
26. Wang, Z.; Pan, X.; Li, L.; Fantin, M.; Yan, J.; Wang, Z.; Wang, Z.; Xia, H.; Matyjaszewski, K. Enhancing Mechanically Induced ATRP by Promoting Interfacial Electron Transfer from Piezoelectric Nanoparticles to Cu Catalysts. *Macromolecules* **2017**, *50*, 7940–7948. [CrossRef]
27. Zaborniak, I.; Chmielarz, P. Ultrasound-Mediated Atom Transfer Radical Polymerization (ATRP). *Materials* **2019**, *12*, 3600. [CrossRef]
28. Pan, X.; Fantin, M.; Yuan, F.; Matyjaszewski, K. Externally Controlled Atom Transfer Radical Polymerization. *Chem. Soc. Rev.* **2018**, *47*, 5457–5490. [CrossRef]
29. Ribelli, T.G.; Lorandi, F.; Fantin, M.; Matyjaszewski, K. Atom Transfer Radical Polymerization: Billion Times More Active Catalysts and New Initiation Systems. *Macromol. Rapid Commun.* **2019**, *40*, 1800616. [CrossRef]
30. De Paoli, P.; Isse, A.A.; Bortolamei, N.; Gennaro, A. New Insights into the Mechanism of Activation of Atom Transfer Radical Polymerization by Cu(I) Complexes. *Chem. Commun.* **2011**, *47*, 3580–3582. [CrossRef] [PubMed]
31. Isse, A.A.; Bortolamei, N.; De Paoli, P.; Gennaro, A. On the Mechanism of Activation of Copper-Catalyzed Atom Transfer Radical Polymerization. *Electrochim. Acta* **2013**, *110*, 655–662. [CrossRef]
32. Fantin, M.; Lorandi, F.; Gennaro, A.; Isse, A.; Matyjaszewski, K. Electron Transfer Reactions in Atom Transfer Radical Polymerization. *Synthesis* **2017**, *49*, 3311–3322. [CrossRef]
33. Penczek, S.; Pretula, J.; Lewiński, P. Dormant Polymers and Their Role in Living and Controlled Polymerizations; Influence on Polymer Chemistry, Particularly on the Ring Opening Polymerization. *Polymers* **2017**, *9*, 646. [CrossRef]
34. Tang, W.; Kwak, Y.; Braunecker, W.; Tsarevsky, N.V.; Coote, M.L.; Matyjaszewski, K. Understanding Atom Transfer Radical Polymerization: Effect of Ligand and Initiator Structures on the Equilibrium Constants. *J. Am. Chem. Soc.* **2008**, *130*, 10702–10713. [CrossRef] [PubMed]
35. Braunecker, W.A.; Tsarevsky, N.V.; Gennaro, A.; Matyjaszewski, K. Thermodynamic Components of the Atom Transfer Radical Polymerization Equilibrium: Quantifying Solvent Effects. *Macromolecules* **2009**, *42*, 6348–6360. [CrossRef]
36. Buback, M.; Morick, J. Equilibrium Constants and Activation Rate Coefficients for Atom Transfer Radical Polymerizations at Pressures up to 2 500 Bar. *Macromol. Chem. Phys.* **2010**, *211*, 2154–2161. [CrossRef]
37. Wang, Y.; Kwak, Y.; Buback, J.; Buback, M.; Matyjaszewski, K. Determination of ATRP Equilibrium Constants under Polymerization Conditions. *ACS Macro Lett.* **2012**, *1*, 1367–1370. [CrossRef]
38. Lorandi, F.; Fantin, M.; Isse, A.A.; Gennaro, A.; Matyjaszewski, K. New Protocol to Determine the Equilibrium Constant of Atom Transfer Radical Polymerization. *Electrochim. Acta* **2018**, *260*, 648–655. [CrossRef]
39. De Bon, F.; Isse, A.A.; Gennaro, A. Electrochemically Mediated Atom Transfer Radical Polymerization of Methyl Methacrylate: The Importance of Catalytic Halogen Exchange. *Chem. Electro. Chem.* **2019**, *6*, 4257–4265. [CrossRef]
40. Chmielarz, P.; Sobkowiak, A.; Matyjaszewski, K. A Simplified Electrochemically Mediated ATRP Synthesis of PEO-b-PMMA Copolymers. *Polymer* **2015**, *77*, 266–271. [CrossRef]
41. Chmielarz, P.; Yan, J.; Krys, P.; Wang, Y.; Wang, Z.; Bockstaller, M.R.; Matyjaszewski, K. Synthesis of Nanoparticle Copolymer Brushes via Surface-Initiated seATRP. *Macromolecules* **2017**, *50*, 4151–4159. [CrossRef]
42. Wang, J.; Tian, M.; Li, S.; Wang, R.; Du, F.; Xue, Z. Ligand-Free Iron-Based Electrochemically Mediated Atom Transfer Radical Polymerization of Methyl Methacrylate. *Polym. Chem.* **2018**, *9*, 4386–4394. [CrossRef]
43. De Bon, F.; Ribeiro, D.C.M.; Abreu, C.M.R.; Rebelo, R.A.C.; Isse, A.A.; Serra, A.C.; Gennaro, A.; Matyjaszewski, K.; Coelho, J.F.J. Under Pressure: Electrochemically-Mediated Atom Transfer Radical Polymerization of Vinyl Chloride. *Polym. Chem.* **2020**, *11*, 6745–6762. [CrossRef]
44. Guo, J.-K.; Zhou, Y.-N.; Luo, Z.-H. Iron-Based Electrochemically Mediated Atom Transfer Radical Polymerization with Tunable Catalytic Activity. *AIChE J.* **2018**, *64*, 961–969. [CrossRef]
45. De Bon, F.; Isse, A.A.; Gennaro, A. Towards Scale-up of Electrochemically-Mediated Atom Transfer Radical Polymerization: Use of a Stainless-Steel Reactor as Both Cathode and Reaction Vessel. *Electrochim. Acta* **2019**, *304*, 505–512. [CrossRef]
46. Zaborniak, I.; Chmielarz, P.; Martinez, M.R.; Wolski, K.; Wang, Z.; Matyjaszewski, K. Synthesis of High Molecular Weight Poly(n-Butyl Acrylate) Macromolecules via seATRP: From Polymer Stars to Molecular Bottlebrushes. *Eur. Polym. J.* **2020**, *126*, 109566. [CrossRef]
47. Chmielarz, P.; Park, S.; Simakova, A.; Matyjaszewski, K. Electrochemically Mediated ATRP of Acrylamides in Water. *Polymer* **2015**, *60*, 302–307. [CrossRef]
48. Fantin, M.; Isse, A.A.; Gennaro, A.; Matyjaszewski, K. Understanding the Fundamentals of Aqueous ATRP and Defining Conditions for Better Control. *Macromolecules* **2015**, *48*, 6862–6875. [CrossRef]
49. Strover, L.T.; Malmström, J.; Stubbing, L.A.; Brimble, M.A.; Travas-Sejdic, J. Electrochemically-Controlled Grafting of Hydrophilic Brushes from Conducting Polymer Substrates. *Electrochim. Acta* **2016**, *188*, 57–70. [CrossRef]
50. Sun, Y.; Lathwal, S.; Wang, Y.; Fu, L.; Olszewski, M.; Fantin, M.; Enciso, A.E.; Szczepaniak, G.; Das, S.; Matyjaszewski, K. Preparation of Well-Defined Polymers and DNA–Polymer Bioconjugates via Small-Volume EATRP in the Presence of Air. *ACS Macro Lett.* **2019**, *8*, 603–609. [CrossRef]

51. Michieletto, A.; Lorandi, F.; De Bon, F.; Isse, A.A.; Gennaro, A. Biocompatible Polymers via Aqueous Electrochemically Mediated Atom Transfer Radical Polymerization. *J. Polym. Sci.* **2020**, *58*, 114–123. [CrossRef]
52. Lorandi, F.; Fantin, M.; Wang, Y.; Isse, A.A.; Gennaro, A.; Matyjaszewski, K. Atom Transfer Radical Polymerization of Acrylic and Methacrylic Acids: Preparation of Acidic Polymers with Various Architectures. *ACS Macro Lett.* **2020**, *9*, 693–699. [CrossRef]
53. Zaborniak, I.; Chmielarz, P.; Matyjaszewski, K. Synthesis of Riboflavin-Based Macromolecules through Low Ppm ATRP in Aqueous Media. *Macromol. Chem. Phys.* **2020**, *221*, 1900496. [CrossRef]
54. De Bon, F.; Marenzi, S.; Isse, A.A.; Durante, C.; Gennaro, A. Electrochemically Mediated Aqueous Atom Transfer Radical Polymerization of *N*,*N*-Dimethylacrylamide. *ChemElectroChem* **2020**, *7*, 1378–1388. [CrossRef]
55. Fantin, M.; Park, S.; Wang, Y.; Matyjaszewski, K. Electrochemical Atom Transfer Radical Polymerization in Miniemulsion with a Dual Catalytic System. *Macromolecules* **2016**, *49*, 8838–8847. [CrossRef]
56. Fantin, M.; Chmielarz, P.; Wang, Y.; Lorandi, F.; Isse, A.A.; Gennaro, A.; Matyjaszewski, K. Harnessing the Interaction between Surfactant and Hydrophilic Catalyst To Control *e*ATRP in Miniemulsion. *Macromolecules* **2017**, *50*, 3726–3732. [CrossRef] [PubMed]
57. Zaborniak, I.; Chmielarz, P. Miniemulsion Switchable Electrolysis under Constant Current Conditions. *Polym. Adv. Technol.* **2020**, *31*, 2806–2815. [CrossRef]
58. De Bon, F.; Fantin, M.; Isse, A.A.; Gennaro, A. Electrochemically Mediated ATRP in Ionic Liquids: Controlled Polymerization of Methyl Acrylate in [BMIm][OTf]. *Polym. Chem.* **2018**, *9*, 646–655. [CrossRef]
59. Guo, J.K.; Zhou, Y.N.; Luo, Z.H. Electrochemically Mediated ATRP Process Intensified by Ionic Liquid: A "Flash" Polymerization of Methyl Acrylate. *Chem. Eng. J.* **2019**, *372*, 163–170. [CrossRef]
60. Wang, J.-S.; Matyjaszewski, K. Controlled/"Living" Radical Polymerization. Halogen Atom Transfer Radical Polymerization Promoted by a Cu(I)/Cu(II) Redox Process. *Macromolecules* **1995**, *28*, 7901–7910. [CrossRef]
61. Matyjaszewski, K.; Patten, T.E.; Xia, J. Controlled/"Living" Radical Polymerization. Kinetics of the Homogeneous Atom Transfer Radical Polymerization of Styrene. *J. Am. Chem. Soc.* **1997**, *119*, 674–680. [CrossRef]
62. Angot, S.; Murthy, K.S.; Taton, D.; Gnanou, Y. Atom Transfer Radical Polymerization of Styrene Using a Novel Octafunctional Initiator: Synthesis of Well-Defined Polystyrene Stars. *Macromolecules* **1998**, *31*, 7218–7225. [CrossRef]
63. Plichta, A.; Li, W.; Matyjaszewski, K. ICAR ATRP of Styrene and Methyl Methacrylate with Ru(Cp*)Cl(PPh 3) 2. *Macromolecules* **2009**, *42*, 2330–2332. [CrossRef]
64. Zhang, L.; Miao, J.; Cheng, Z.; Zhu, X. Iron-Mediated ICAR ATRP of Styrene and Methyl Methacrylate in the Absence of Thermal Radical Initiator. *Macromol. Rapid Commun.* **2010**, *31*, 275–280. [CrossRef] [PubMed]
65. Mukumoto, K.; Wang, Y.; Matyjaszewski, K. Iron-Based ICAR ATRP of Styrene with Ppm Amounts of Fe III Br 3 and 1,1′-Azobis(Cyclohexanecarbonitrile). *ACS Macro Lett.* **2012**, *1*, 599–602. [CrossRef]
66. Jakubowski, W.; Matyjaszewski, K. Activator Generated by Electron Transfer for Atom Transfer Radical Polymerization. *Macromolecules* **2005**, *38*, 4139–4146. [CrossRef]
67. Jakubowski, W.; Min, K.; Matyjaszewski, K. Activators Regenerated by Electron Transfer for Atom Transfer Radical Polymerization of Styrene. *Macromolecules* **2006**, *39*, 39–45. [CrossRef]
68. Jakubowski, W.; Kirci-Denizli, B.; Gil, R.R.; Matyjaszewski, K. Polystyrene with Improved Chain-End Functionality and Higher Molecular Weight by ARGET ATRP. *Macromol. Chem. Phys.* **2008**, *209*, 32–39. [CrossRef]
69. Braidi, N.; Buffagni, M.; Ghelfi, F.; Imperato, M.; Menabue, A.; Parenti, F.; Gennaro, A.; Isse, A.A.; Bedogni, E.; Bonifaci, L.; et al. Copper-Catalysed "Activators Regenerated by Electron Transfer" "Atom Transfer Radical Polymerisation" of Styrene from a Bifunctional Initiator in Ethyl Acetate/Ethanol, Using Ascorbic Acid/Sodium Carbonate as Reducing System. *Macromol. Res.* **2020**, *28*, 751–761. [CrossRef]
70. Braidi, N.; Buffagni, M.; Buzzoni, V.; Ghelfi, F.; Parenti, F.; Focarete, M.L.; Gualandi, C.; Bedogni, E.; Bonifaci, L.; Cavalca, G.; et al. Unusual Cross-Linked Polystyrene by Copper-Catalyzed ARGET ATRP Using a Bifunctional Initiator and No Cross-Linking Agent. *Macromol. Res.* **2021**, *29*, 280–288. [CrossRef]
71. Hsiao, C.-Y.; Han, H.-A.; Lee, G.-H.; Peng, C.-H. AGET and SARA ATRP of Styrene and Methyl Methacrylate Mediated by Pyridyl-Imine Based Copper Complexes. *Eur. Polym. J.* **2014**, *51*, 12–20. [CrossRef]
72. Mendes, J.P.; Góis, J.R.; Costa, J.R.C.; Maximiano, P.; Serra, A.C.; Guliashvili, T.; Coelho, J.F.J. Ambient Temperature SARAATRP for Meth(Acrylates), Styrene, and Vinyl Chloride Using Sulfolane/1-Butyl-3-Methylimidazolium Hexafluorophosphate-Based Mixtures. *J. Polym. Sci. Part A Polym. Chem.* **2017**, *55*, 1322–1328. [CrossRef]
73. Chmielarz, P.; Krol, P. PSt-b-PU-b-PSt Copolymers Using Tetraphenylethane-Urethane Macroinitiator through SARA ATRP. *Express Polym. Lett.* **2016**, *10*, 302–310. [CrossRef]
74. Whitfield, R.; Anastasaki, A.; Nikolaou, V.; Jones, G.R.; Engelis, N.G.; Discekici, E.H.; Fleischmann, C.; Willenbacher, J.; Hawker, C.J.; Haddleton, D.M. Universal Conditions for the Controlled Polymerization of Acrylates, Methacrylates, and Styrene via Cu(0)-RDRP. *J. Am. Chem. Soc.* **2017**, *139*, 1003–1010. [CrossRef] [PubMed]
75. Liu, X.; Zhang, L.; Cheng, Z.; Zhu, X. Metal-Free Photoinduced Electron Transfer–Atom Transfer Radical Polymerization (PET–ATRP) via a Visible Light Organic Photocatalyst. *Polym. Chem.* **2016**, *7*, 689–700. [CrossRef]
76. Kütahya, C.; Schmitz, C.; Strehmel, V.; Yagci, Y.; Strehmel, B. Near-Infrared Sensitized Photoinduced Atom-Transfer Radical Polymerization (ATRP) with a Copper(II) Catalyst Concentration in the Ppm Range. *Angew. Chemie Int. Ed.* **2018**, *57*, 7898–7902. [CrossRef] [PubMed]

77. Su, C.; Wu, Z.; Lin, C.; Han, H.; Chen, Y.; Chou, P.; Fu, X.; Peng, C. Polystyrene with Persistently Enhanced Fluorescence: Photo-Induced Atom Transfer Radical Polymerization Using a Pyrene-Based Initiator. *Chem. Photo. Chem.* **2019**, *3*, 1153–1161. [CrossRef]
78. Bonometti, V.; Labbé, E.; Buriez, O.; Mussini, P.; Amatore, C. Exploring the First Steps of an Electrochemically-Triggered Controlled Polymerization Sequence: Activation of Alkyl- and Benzyl Halide Initiators by an Electrogenerated FeIISalen Complex. *J. Electroanal. Chem.* **2009**, *633*, 99–105. [CrossRef]
79. Buback, M.; Gilbert, R.G.; Hutchinson, R.A.; Klumperman, B.; Kuchta, F.-D.; Manders, B.G.; O'Driscoll, K.F.; Russell, G.T.; Schweer, J. Critically Evaluated Rate Coefficients for Free-Radical Polymerization, 1. Propagation Rate Coefficient for Styrene. *Macromol. Chem. Phys.* **1995**, *196*, 3267–3280. [CrossRef]
80. Nicholson, R.S. Theory and Application of Cyclic Voltammetry for Measurement of Electrode Reaction Kinetics. *Anal. Chem.* **1965**, *37*, 1351–1355. [CrossRef]
81. Fawcett, W.R.; Opallo, M. The Kinetics of Heterogeneous Electron Transfer Reaction in Polar Solvents. *Angew. Chem. Int. Ed. Engl.* **1994**, *33*, 2131–2143. [CrossRef]
82. Pavan, P.; Lorandi, F.; De Bon, F.; Gennaro, A.; Isse, A.A. Enhancement of the Rate of Atom Transfer Radical Polymerization in Organic Solvents by Addition of Water: An Electrochemical Study. *Chem. Electro. Chem.* **2021**, *8*, 2450–2458. [CrossRef]
83. Bortolamei, N.; Isse, A.A.; Di Marco, V.B.; Gennaro, A.; Matyjaszewski, K. Thermodynamic Properties of Copper Complexes Used as Catalysts in Atom Transfer Radical Polymerization. *Macromolecules* **2010**, *43*, 9257–9267. [CrossRef]
84. Zerk, T.J.; Bernhardt, P.V. Organo-Copper(II) Complexes as Products of Radical Atom Transfer. *Inorg. Chem.* **2017**, *56*, 5784–5792. [CrossRef] [PubMed]
85. Fantin, M.; Lorandi, F.; Ribelli, T.G.; Szczepaniak, G.; Enciso, A.E.; Fliedel, C.; Thevenin, L.; Isse, A.A.; Poli, R.; Matyjaszewski, K. Impact of Organometallic Intermediates on Copper-Catalyzed Atom Transfer Radical Polymerization. *Macromolecules* **2019**, *52*, 4079–4090. [CrossRef]